

**Teilprojekt B3.03**

## **Modeling of Quantum Information Devices**

**Principal Investigator: Alexander Shnirman, Gerd Schön**

**CFN financed scientists: Pablo San Jose (26 months), Stephan André (25 months 0,75),  
Clemens Müller (6 month 0.5 + 12 months 0,75)**

**Further contributing scientists: Valentina Brosco, Jared Cole, Michael Marthaler, Simone  
Montangero, Lin Tian, Pei-Qing Jin, Alessandro Romito**

**Institut für Theoretische Festkörperphysik  
Karlsruhe Institute of Technology**

**Institut für Theorie der Kondensierten Materie  
Karlsruhe Institute of Technology**

## Quantum information devices

Quantum state engineering, i.e., active control over the coherent dynamics of suitable quantum mechanical systems, opens fascinating perspectives for the future of quantum information processing. For this purpose a number of individual two-state quantum systems (qubits) should be manipulated in a controlled way. Nano-electronic devices appear particularly promising because they can be embedded in electronic circuits and scaled up to large numbers of qubits.

Two clearly leading proposals for realization of qubits in nano-electronic devices are Josephson circuits and spins in quantum dots. After initial breakthroughs in 1999-2002 the Josephson qubit technology has reached today a stage where all possible single-bit and many two-bit operations can be performed. Recently a new field 'circuit QED' has emerged where Josephson qubits strongly coupled to microwave resonators are investigated. In circuit QED many effects initially discussed in quantum electrodynamics and atomic physics have been clearly observed, e.g., vacuum Rabi oscillations, ac Stark shift, quantum non-demolition measurements, geometric phases, lasing and cooling. Moreover, superconducting qubits have been used as measurement devices, e.g., to perform spectroscopy on material dependent impurities.

Spins in quantum dots have also shown great progress in recent years. Single spin manipulations have been performed, singlet-triplet qubits in double quantum dots have been realized, the role of nuclear spin environment has been appreciated, and long echo times of order  $1\mu\text{s}$  have been observed.

Motivated by these achievements we pursued the following projects:

- Characterization of noise in qubits from experimental data.
- Properties of  $1/f$  noise and two-level fluctuators.
- Coupling of Josephson qubits.
- Circuit QED, lasing and cooling with Josephson qubits.
- Ballistic readout of flux qubits.
- Spatial adiabatic passage in a realistic triple well structure.
- Geometric manipulations of spins.
- Fault-tolerant qubit systems.

Much of our work is done in close interaction with experimental groups within the CFN and outside. With some of them we cooperate in the frame of European networks.

### 1. Characterization of noise in qubits from experimental data.

Decoherence in quantum bit circuits is presently a major limitation to their use for quantum computing purposes. It is very important to characterize the noise causing decoherence in order to minimize its effect. In collaboration with the experimental group in NTT (Japan) we analyzed [B3.3:5] decoherence in a flux qubit. They measured the magnetic field dependence of the characteristic energy relaxation time ( $T_1$ ) and echo phase relaxation time ( $T_2^{\text{echo}}$ ) near the optimal operating point of a flux qubit. At the optimal point, the relation  $T_2^{\text{echo}} \sim 2 T_1$  was observed, i.e., the echo decay time is limited by the energy relaxation. Moving away from the optimal point, a *linear* increase of the phase relaxation rate  $1/T_2^{\text{echo}}$  with the applied external magnetic flux was observed. This behavior can be well explained by the influence of magnetic flux noise with a  $1/f$  spectrum on

the qubit. We have extracted the amplitude of the  $1/f$  flux noise and confirmed that it is close to the “universal” value observed in many other experiments,  $\sim 10^{-6} \Phi_0$ .

## 2. Properties of $1/f$ noise and two-level fluctuators.

$1/f$  noise is the major source of dephasing in Josephson qubits. We have investigated the microscopic models of  $1/f$  noise, in particular the models where the noise is produced by a bath of two-level fluctuators.

We investigated the statistical properties of  $1/f$  noise produced by an ensemble of two-level systems [B3.3:1]. Depending on the two-level fluctuators’ distribution, the noise distribution can be Gaussian or non-Gaussian. The latter situation is realized, for instance, when the distribution of coupling strengths has a slowly decaying power-law tail. In this regime questions of self-averaging and sample-to-sample fluctuations become crucial. We studied the dephasing process for a class of distribution functions and analyzed the self-averaging properties of the results.

We introduced a wide class of non-trivial quantum spin baths which embrace Ising, XY, and Heisenberg universality classes coupled to a two-level system and determined the decoherence rates [B3.3:12]. For the XY and Ising universality classes we provided an exact expression for the decay of the loss of coherence beyond the case of a central spin coupled uniformly to all the spins of the baths, which has been discussed so far in the literature. In the case of the Heisenberg spin bath we studied decoherence by means of the time-dependent density matrix renormalization group. We showed how these baths can be engineered by using atoms in optical lattices.

## 3. Coupling of Josephson and spin qubits.

We analyzed the coupling of qubits mediated by a tunable and fast element beyond the adiabatic approximation [B3.3:2]. The nonadiabatic corrections are important and even dominant in parts of the relevant parameter range. As an example, we considered the tunable capacitive coupling between two charge qubits mediated by a gated Josephson junction (see Fig. 1), as suggested by Averin and Bruder. The nonadiabatic, inductive contribution persists when the capacitive coupling is tuned to zero. On the other hand, the total coupling can be turned off (in the rotating wave approximation) if the qubits are operated at symmetry points.

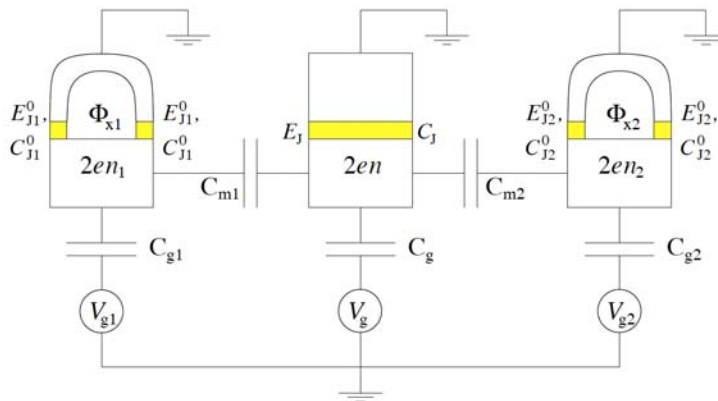


**Fig. 1.** Two charge qubits coupled via a single-Cooper-pair box.

For inductively coupled superconducting quantum bits, we determined the conditions when the coupling commutes with the single-qubit terms [B3.3:8]. We showed that in certain parameter

regimes such longitudinal coupling can be stabilized with respect to variations of the circuit parameters. In addition, we analyzed its stability against fluctuations of the control fields.

In addition to the work on Josephson qubits, we have studied aspects of the coupling between spin-qubits [B3.3:24]. Specifically, we considered the effect of charge-fluctuations during the realization of an entangling operation via the exchange interaction. As the exchange interaction stems from the wavefunction overlap between two spins, charge fluctuations in the surrounding environment will result in fluctuations in the coupling strength. We developed an analytical model for such fluctuations, which applies at all timescales of the charge noise.

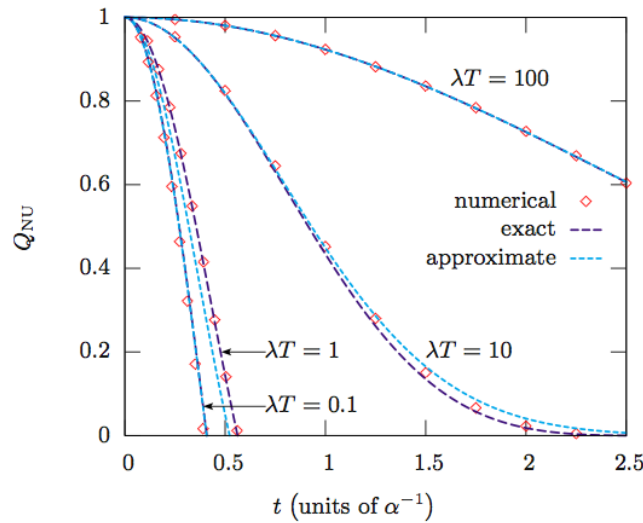


**Fig. 2.** Magnitude of the non-zero elements of the two-spin exchange superoperator for various fluctuation rates, computed numerically as well as analytically (both approximate and exact).

#### 4. Circuit QED, lasing and cooling with Josephson qubits.

Coupling of the Josephson qubits to resonators brought superconducting circuits into the realm of quantum electrodynamics (“circuit QED”) [A. Wallraff *et al.*, Nature **431**, 162 (2004), I. Chiorescu *et al.*, Nature **431**, 159 (2004)]. It opened the perspective to use superconducting qubits as micro-coolers or to create a population inversion in the qubit to induce lasing behavior of the resonator.

Motivated by experiments performed in Jena we considered an ac-driven qubit coupled to a low-frequency LC-circuit [B3.3:15,B3.3:20,B3.3:21]. When the qubit is driven to perform Rabi oscillations, with Rabi frequency in resonance with the oscillator, the latter can be driven far from equilibrium. Blue detuned driving leads to a population inversion in the qubit and lasing behavior of the oscillator (“single-atom laser”). For red detuning the qubit cools the oscillator. This behavior persists at the symmetry point where the qubit-oscillator coupling is quadratic and decoherence effects are minimized. Here the system realizes a “single-atom-two-photon laser”. Interestingly the population inversion typical for the lasing is induced in the dressed state basis. It arises as a consequence of the pumping and relaxation processes in the lab frame.

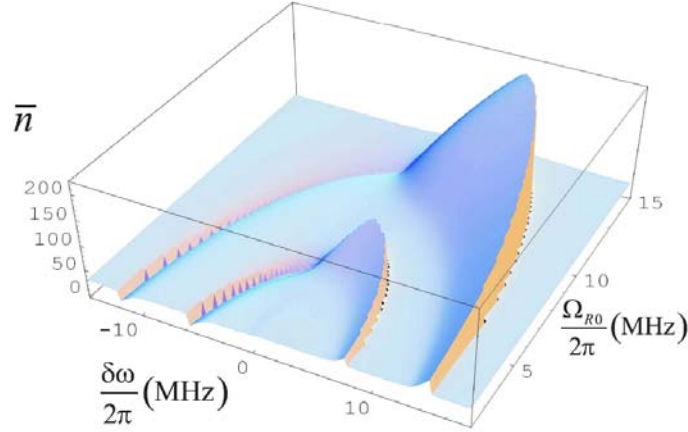


**Fig. 3.** Average number of photons in the resonator as function of the driving detuning  $\delta\omega$  and amplitude  $\Omega_{R0}$ . Peaks at  $\delta\omega > 0$  correspond to lasing, while dips at  $\delta\omega < 0$  correspond to cooling. The inner curve corresponds to the one-photon resonance which exists only away from the symmetry point. The outer curve describes the two-photon resonance, which persists at the symmetry point. In domains of bistability the lowest value of  $n$  is plotted (leading to the sharp drops in both curves).

Furthering the analogies between optical and circuit QED, we demonstrated in Ref. [B3.3:14] Sisyphus cooling and amplification of a low frequency LC oscillator coupled to a near-resonantly driven superconducting qubit. In the quantum optics setup the mechanical oscillations of an atom are cooled or amplified by laser driving the atom's electronic degrees of freedom. Here, the roles of the two degrees of freedom are played by the LC circuit and the qubit's levels, respectively. Red-detuned high-frequency driving of the qubit produces cooling of the resonator, while blue detuning leads to the opposite, namely Sisyphus amplification, which is a precursor of lasing with the characteristic line-width narrowing. Parallel to the experimental demonstration of these processes we analyzed the system theoretically. The good agreement with experiment confirms our interpretation and allows us to estimate system parameters.

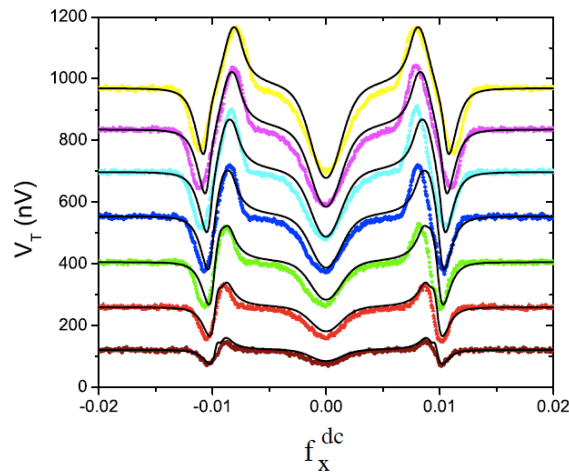


**Fig. 4.** Sisyphus cooling and lasing. Voltage at the low frequency LC resonator in response to a resonant driving for seven different driving amplitudes. Maxima correspond to enhancement of the effective quality factor, i.e., to amplification/lasing. Minima at the sides (near the maxima) correspond to cooling. Color lines are the experiment, black lines the theory.

Motivated by recent experiments [B3.3:14, O. Astafiev *et al.*, Nature **449**, 588 (2007)], which demonstrated lasing and cooling of the electromagnetic field in a high-frequency electrical resonator coupled to a superconducting qubit, we studied in Refs. [B3.3:23,B3.3:27,B3.3:31] the phase coherence of the system in the lasing state. We considered phase locking and synchronization induced by an additional driving of the resonator. Our theory extends earlier work in the field of quantum optics to a wide parameter range, incl. the regime of strong coupling, and to a low number of “atoms”. We also included the effects of low-frequency noise in our model. The resulting width and shape of the spectrum are consistent with those measured in the experiment [O. Astafiev *et al.*, Nature **449**, 588 (2007)].

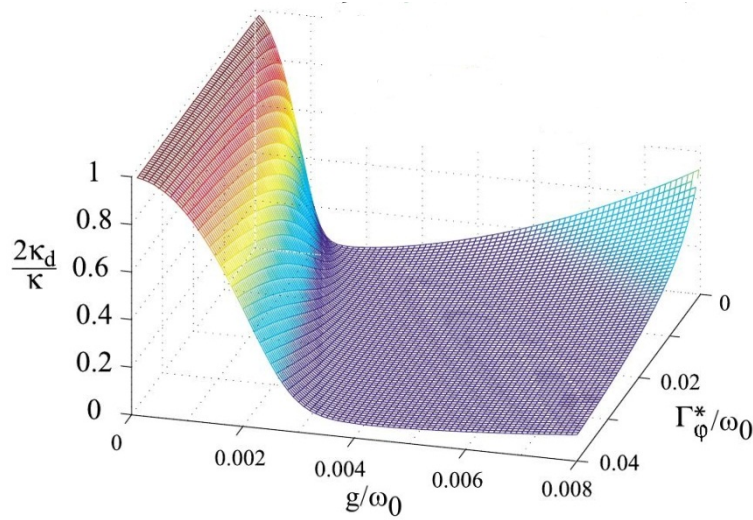


**Fig. 5:** Width of the resonator emission spectrum as function of the coupling strength  $g$  and pure dephasing rate  $\Gamma_\phi^*$ . In the strong coupling regime, an increasing pure dephasing of the qubit may lead to a *smaller* linewidth.

Single-qubit lasers can show interesting behavior and pronounced effects when the frequency of the qubit and the resonator are detuned. This was shown in Ref. [B3.3:35], where the spectral properties of single-qubit lasers are investigated as a function of the detuning in the regime of (very) strong coupling between qubit and resonator. By using an approach based on a Fokker-Planck equation for the laser field, we derived analytical results showing that this is due to a coupling of amplitude and phase fluctuations of the electrical field, usually neglected in conventional laser theories.

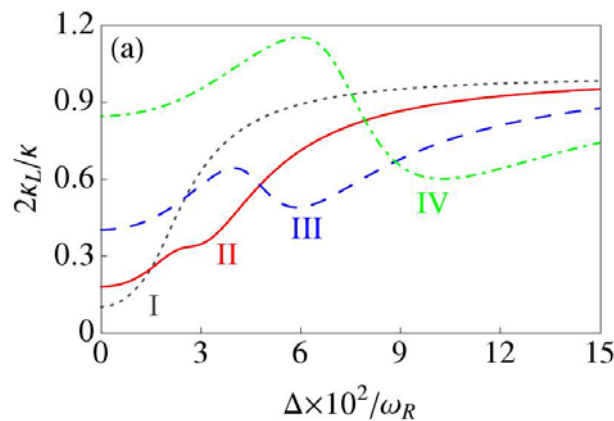


**Fig. 6:** Laser linewidth as function of the detuning  $\Delta$  between qubit and resonator. The curves I-IV correspond to increasing coupling strength. For strong (fixed) coupling, a strong enhancement of the linewidth can be observed at the lasing transition.

We proposed in Ref. [3.3:19] a way to create strongly squeezed photon number states in a system consisting of superconducting single-electron transistor (SSET) coupled to an anharmonic oscillator, e.g., a Josephson junction-LC circuit. By biasing the SSET in a regime where the current is carried by a combination of inelastic quasiparticle tunneling and coherent Cooper-pair tunneling (Josephson quasiparticle cycle), cooling of the oscillator as well as a laser-like enhancement of the photon number can be achieved. We showed that the cut-off in the quasiparticle tunneling rate due to the superconducting gap, in combination with the anharmonicity of the oscillator, may create strongly squeezed photon number states. For low dissipation in the oscillator nearly pure Fock states can be produced.

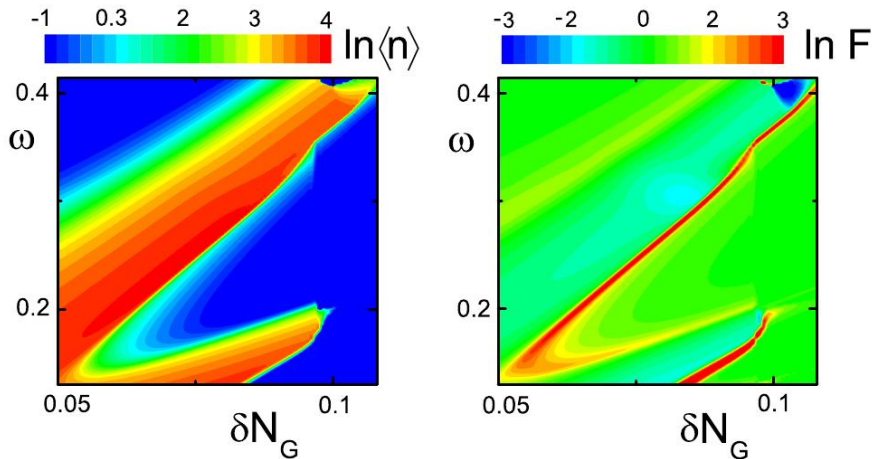


**Fig. 7:** Average photon number (left picture) in the resonator and Fano factor (right picture) as functions of the oscillator frequency  $\omega$  and the gate charge  $N_g$ .

### 5. Ballistic readout of flux qubits.

We described [B3.3:7, B3.3:13] a measurement process of a flux qubit by Josephson solitons in the dissipative underdamped Josephson Transmission Lines (JTL). The JTL is a standard element of the RSFQ technology and our work should assess the feasibility of combining the Josephson qubits with the RSFQ elements. We considered the limit in which the information about the state of the qubit is stored in the time delay experienced by the soliton. We took into account the JTL jitter and provided estimates for the measuring time at relevant experimental parameters.

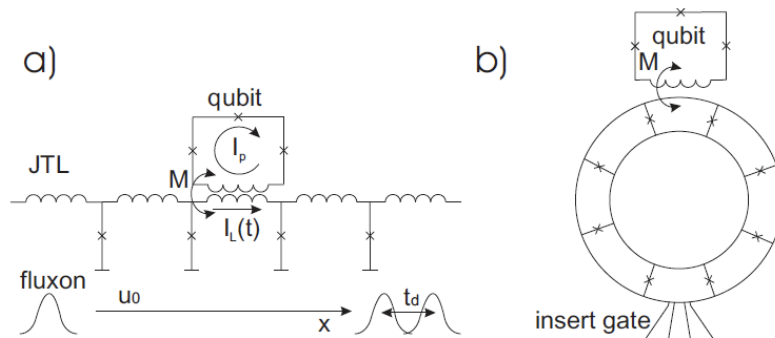


**Fig. 8.** a) Setup for the read-out of the persistent current qubit based on the delay time of a soliton in the Josephson transmission line (JTL); b) circular setup for multiple scattering of solitons on the qubit.

## 6. Spatial adiabatic passage in a realistic triple well structure.

We investigated the evolution of an electron undergoing coherent tunneling via adiabatic passage (CTAP) using the solution of the one-dimensional Schrödinger equation in both space and time for a triple well potential. We found the eigenspectrum and complete time evolution for a range of different pulsing schemes. This also provides an example of a system that can be described with the tools from both quantum optics and condensed matter. We found that while the quantum optics description of the process captured most of the key physics, there were important effects that could only be correctly described by a more complete representation. This is an important point for applications such as quantum information processing or quantum control where it is common practice to use a reduced state space formulation of the quantum system in question.

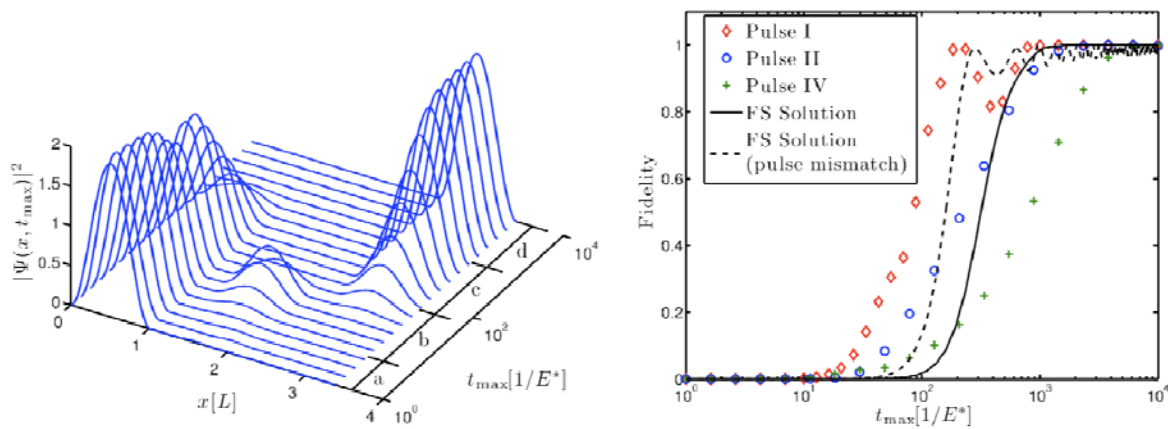


**Fig. 9.** a) Probability distribution as a function of pulse time for a completed CTAP sequence, illustrating the cross-over from diabatic to adiabatic evolution. b) Fidelity of transfer as a function of pulse time for various pulsing schemes, using both finite state (FS) and one-dimensional Schrödinger evolution.

## 7. Geometric manipulations of spins.

In [B3.3:16], in addition to studying the relaxation of spin as reported in the report for the subproject B2.2, we have suggested a way to manipulate the quantum state of a spin qubit by applied electric fields only. The electric fields can be used via the spin-orbit interaction to control the geometric phases, which allows performing quantum coherent spin manipulations without using high-frequency magnetic fields.

## 8. Fault-tolerant qubit systems.

We described [B3.3:9] a qubit encoded in continuous quantum variables of an rf superconducting quantum interference device. Since the number of accessible states in the system is infinite, we may protect its two-dimensional subspace from small errors introduced by the interaction with the environment and during manipulations. We showed how to prepare the fault-tolerant state and manipulate the system. The discussed operations suffice to perform quantum computation on the encoded state, syndrome extraction, and quantum error correction. We also commented on the physical sources of errors and possible imperfections while manipulating the system.

Quantum optimal control theory allows us to design accurate quantum gates. We employed it [B3.3:10] to design high-fidelity two-bit gates for Josephson charge qubits in the presence of both leakage and noise. Our protocol considerably increases the fidelity of the gate and, more important, it is quite robust in the disruptive presence of  $1/f$  noise. The improvement in the gate performances discussed in this work (errors  $\sim 10^{-3}$ – $10^{-4}$  in realistic cases) allows us to cross the fault tolerance threshold.

### 9. Interaction between phase-qubits and two-level fluctuators.

Superconducting qubits often show signatures of coherent coupling to microscopic two-level systems (TLSs), which manifest themselves as avoided level crossings in spectroscopic data. TLS are possibly formed by atomic defects residing inside the amorphous layer of the qubits Josephson junction, but their exact physical nature remains unsolved.

We investigated the energy relaxation (T1) process of a qubit coupled to a bath of dissipative two-level systems. We consider the fluctuators strongly coupled to the qubit both in the limit of spectrally sparse single TLSs as well as in the limit of spectrally dense TLSs. We conclude that the avoided level crossings, usually attributed to very strongly coupled single TLSs, could also be caused by many weakly coupled spectrally dense fluctuators [B3.3:22].

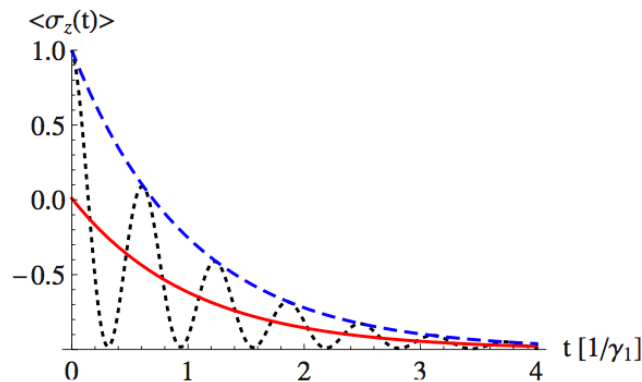
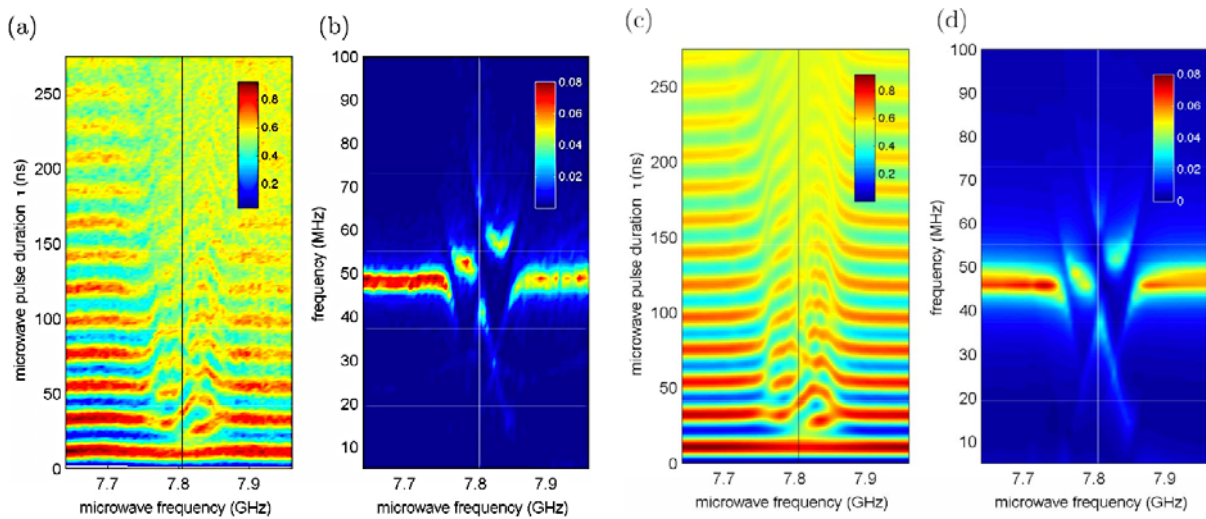


Fig. 10: Decay of the probability to find the qubit in the excited state when it is strongly coupled to a coherent, dissipative TLS (black dotted line). In resonance the two systems show coherent energy exchange and we see oscillations of the probability. Red and blue lines show the extracted effective decoherence envelopes, used to define effective relaxation rates.

In close collaboration with the experimental group of A. V. Ustinov we have tried to elucidate the microscopic origin of the TLS as well as characterize their usefulness for QC tasks. To this end, we studied a phase qubit, in which we induce Rabi oscillations by resonant microwave driving. When the qubit is tuned close to the resonance with an individual TLF and the Rabi driving is strong enough (Rabi frequency of order of the qubit-TLF coupling), interesting four-level dynamics are observed. The experimental data show a clear asymmetry between biasing the qubit above or below the fluctuator's level splitting. Theoretical analysis indicates that this asymmetry is due to an effective coupling of the TLF to the external microwave field induced by the higher qubit levels [B3.3:29].



Fig

Fig. 11: Experimental (left) and theoretical (right) results for Rabi-spectroscopy in a phase qubit coupled to a coherent two-level system.

We also demonstrated a new method to directly manipulate the state of individual two-level systems in phase qubits. It allows one to characterize the coherence properties of TLS using standard microwave pulse sequences, while the qubit is used only for state readout. We applied this method to measure the temperature dependence of TLS coherence. The energy relaxation time  $T_1$  is found to decrease quadratically with temperature for the two TLS studied in this work, while their dephasing time measured in Ramsey and spin-echo experiments is found to be  $T_1$  limited at all temperatures [B3.3:36].

We analysed multiphoton spectroscopy data of a superconducting phase qubit coherently coupled to an intrinsic two-level system. We directly probe hybridized states of the combined qubit-TLS system in the strongly interacting regime, where both the qubit-TLS coupling and the driving cannot be considered as weak perturbations. This regime is described by a theoretical model, which incorporates anharmonic corrections, multiphoton processes and decoherence. Comparison between experiment and theory finds excellent agreement over a wide range of parameters [B3.3:34].

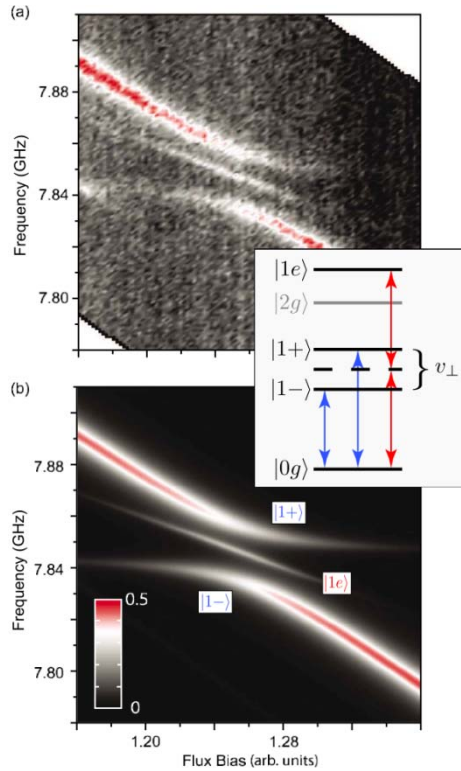


Fig. 12: Experimental (top) and theoretical (bottom) results from spectroscopy of a superconducting phase qubit strongly coupled to a coherent TLS. The inset gives an illustration of the level-structure of the coupled system in resonance as well as indicating the possible transitions in the system. The faint line in the middle of the anticrossing is due to a two-photon transition from the ground- to the fully excited state. Its exact position can be used to shed light on the nature of the coupling between qubit and TLS.

We used high-precision spectroscopy data and detailed theoretical modelling to determine the form of the coupling between a superconducting phase qubit and a two-level defect. Fitting the experimental data with our theoretical model allows us to determine all relevant system parameters. A strong qubit-defect coupling is observed, with a nearly vanishing longitudinal component. Using these estimates, we quantitatively compare several existing theoretical models for the microscopic origin of two-level defects [B3.3:37].

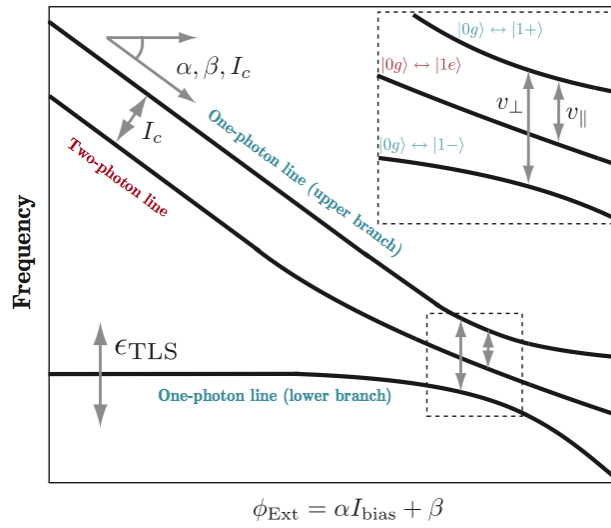


Fig. 13: Illustration of the effects of the multiple parameters of qubit and TLS and their coupling operator on the form of an anticrossing. Fitting to a theoretical model can give strong bounds on the existing theoretical models.

Further topics, currently under investigation include the interplay between multilevel and temperature effects in phase qubits and their influence of the measured decoherence times of two-level fluctuators as well as the use of three-level systems as a more flexible probe of a decohering environment.

## 10. Using qubits as probes of a decohering environment.

The use of qubits as sensitive nanoscale magnetometers has been studied theoretically and recently demonstrated experimentally. We proposed a new concept[B3.3:26], in which a scanning two-state quantum system is used to probe a sample through the subtle effects of decoherence. Mapping both the Hamiltonian and decoherence properties of a qubit simultaneously provides a unique image of the magnetic (or electric) field properties at the nanoscale. The resulting images are sensitive to the temporal as well as spatial variation in the fields created by the sample.

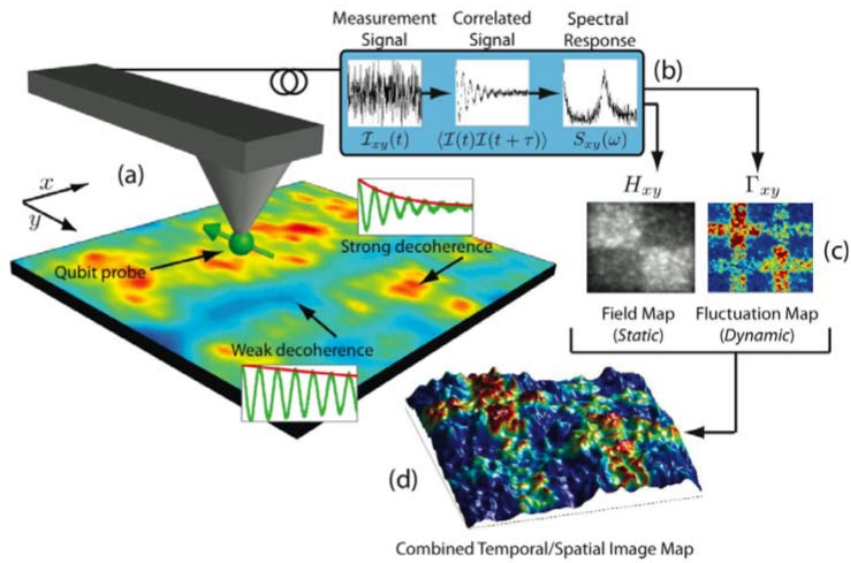


Fig 14. The concept of a decoherence microscope. The properties of a two-state “probe” are monitored as a function of scanning position above a sample. The resulting image provides information about both the static and dynamic properties of the probes environment.

This concept has been further developed to specifically take advantage of the unique properties of NV-centre qubits. Particularly, we have investigated the use of dynamica decoupling for improved sensitivity[B3.3:33], dephasing as a measure of field fluctuations[B3.3:28] and the application of such decoherence probes to biological sensing[B3.3:32].

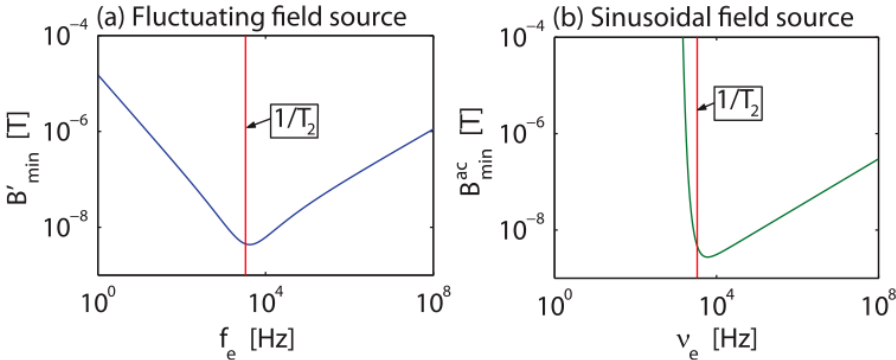


Fig. 15: Comparison of the sensitivity of a NV-centre nanomagnetometer when sensing fluctuating (a) and oscillatory (b) magnetic fields.

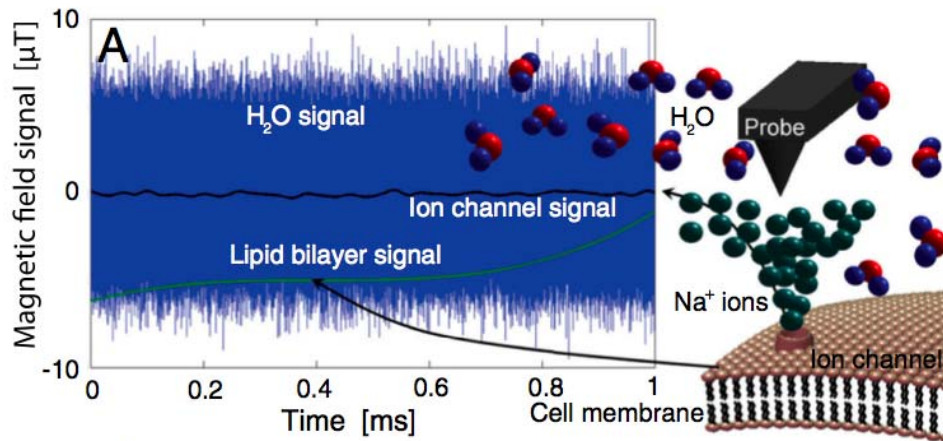


Fig. 16: Simulated detection signal for an NV-centre probe in the vicinity of an operational cell membrane ion-channel, demonstrating the detection of ion-channel switching, even in the presence of a strong fluctuating signal due to nearby water molecules.

We are continuing our investigation into the topic of decoherence microscopy, including the use of a dual-probe configuration for studying partially coherent embedded two-level fluctuators and the cross-over from Markovian to non-Markovian behaviour.